AEGC Australasian Exploration Geoscience Conference Brisbane 2021

Interpretation of magnetotelluric and airborne electromagnetic inversions from the Proterozoic basins of the Capricorn Orogen, WA

Sasha Banaszczyk
Centre for Exploration Targeting, University of Western Australia
35 Stirling Hwy, Crawley, WA
sasha.banaszczyk@gmail.com

Mike Dentith
Centre for Exploration Targeting, University of Western Australia
35 Stirling Hwy, Crawley, WA
michael.dentith@uwa.edu.au

Perla Piña-Varas
Departament de Dinàmica de la Terra i dels Oceans, Universitat de Barcelona
Gran Via de les Corts Catalanes, 585, 08007 Barcelona, Spain
perla.pinavaras@uwa.edu.au

David Annetts
CSIRO
26 Dick Perry Ave, Kensington, WA
david.annetts@csiro.au

SUMMARY

Recently, a regional-scale TEMPEST AEM survey and a local-scale MT survey were acquired over the Yerrida Basin in the Capricorn Orogen, WA. These two electromagnetic datasets provide an opportunity to compare the electromagnetic responses from both the near surface and deeper sedimentary packages within a basin terrain. Both a 3D ModEM inversion of the new MT survey data, and a 1D GA-LEI inversion of a single survey line from the AEM survey data over the Yerrida Basin were jointly interpreted to validate current knowledge of the basin geology. It was found that both the MT and AEM results did not resolve contrasting resistivity variations associated with craton scale structures. However, the new 3D MT inversion, and to a lesser extent the 1D AEM inversion, were useful for interpreting the detailed local-scale faulting and folding of the Yerrida Basin sediments.

Key words: Airborne electromagnetics, Magnetotellurics, Geological interpretation, Capricorn Orogen.

INTRODUCTION

The Yerrida Basin in the south-eastern Capricorn Orogen, WA, hosts locally conformable sedimentary sequences which can be mapped using airborne electromagnetic (AEM) and magnetotelluric (MT) techniques. Few studies compare results from AEM and MT surveys, however, a regional TEMPEST AEM survey over the Capricorn Orogen in addition to a newly acquired MT survey line over the Yerrida Basin provide an opportunity to compare the electromagnetic responses from the near surface and deeper sedimentary packages of the basin.

The regional scale AEM survey was acquired in 2013, covering a survey region of 146,300 km2 across the Capricorn Orogen. This survey formed part of the Western Australian Government's Exploration Incentive Scheme, contributing to the Distal Footprints of Giant Ore Systems: UNCOVER Australia project (Geoscience Australia, 2014; Aitken et al., 2015). Separately, two new local-scale MT survey lines were acquired across the Yerrida and Bryah Basins of the Capricorn Orogen, and were jointly interpreted in conjunction with the regional AEM data. For conciseness we present the results from one of these MT survey lines, and one of the AEM lines acquired over the oldest basin units of the Yerrida Basin.

Regional and widely-spaced AEM surveys are becoming commonplace across sedimentary basin terrains within Australia (Aitken et al., 2015; Folkes, 2017; Brodie and Ley-Cooper, 2018). These surveys are typically inverted with 1D inversion algorithms, however, few of these inversion outputs have been interpreted in conjunction with additional electromagnetic datasets, specifically, MT datasets, to improve on the AEM techniques shallow depth of investigation. In fact, Crowe et al. (2013) and Folkes (2017) have presented the only integrated electromagnetic studies of AEM data with coincident and offline MT surveys.

Folkes (2017) found that robust interpretations of both shallow cover units and deeper crustal features could be achieved through the joint interpretation of both AEM and MT datasets from the Palaeozoic basement rocks and Jurassic to Cretaceous basin sequences of the Thomson Orogen in north-western NSW, and south-western QLD. Folkes (2017) found that the resistivity and thickness variations were vastly different between each inverted data type and that comparison of the two different inversions offered an opportunity to understand the limitations of each electromagnetic surveying method. Generally, there was an overall agreement between the AEM and MT inversion sections, however, cover thicknesses were unreliably recovered in both datasets (Folkes, 2017). Separately, Crowe et al. (2013) used coincident TEMPEST AEM data within 2D MT inversions to constrain the near-surface resistivity variations associated with the conductive Mesoproterozoic sedimentary basins of the Cariewerloo Basin overlying the eastern Gawler Craton, SA. Crowe et al. (2013) found that their MT inversion constrained by AEM data produced results with detailed lateral metre to kilometre scale resistivity variations to approximately 300 m below the surface, which were useful for interpreting faults and unconformities within the basin. The resistivity variations at depths below 300 m were less detailed where the AEM data was unavailable and the inversion only relied on the responses from the relatively widely spaced (1 km spacings) MT survey (Crowe et al., 2013).

Geological Background

The electromagnetic surveys presented here cover the oldest sedimentary packages of the Yerrida Basin. The units which comprise these packages include: the interbedded fine siltstones and sandstones, and dolomitic stromatolite and evaporite sequences of the Juderina Formation (JF), the overlying graphitic and pyritic black shales of the Johnson Cairn Formation (JCF), and the younger turbiditic successions of quartz wackes, intercalated siltstones, shales and dolomites of the Thaduna Formation (TF) (Pirajno and Occhipinti, 2000; Occhipinti et al., 2017). The northern boundary of the Yerrida Basin is in structural contact with the Archean Marymia Inlier at the Jenkin Fault. Recently acquired hand sample resistivities

(Banaszczyk, 2019) from the JCF and JF of the Yerrida Basin have shown that the JCF is a highly conductive unit with a main mode of 2 Ωm, and depending on its thickness within the basin, might be resolved as a large conductor within the AEM and MT inversions. In contrast, the JF is a mostly resistive unit with a main resistivity mode of approximately 5000 Ωm, but also includes a small percentage of conductive interbedded siltstone and sandstone sequences (Banaszczyk, 2019).

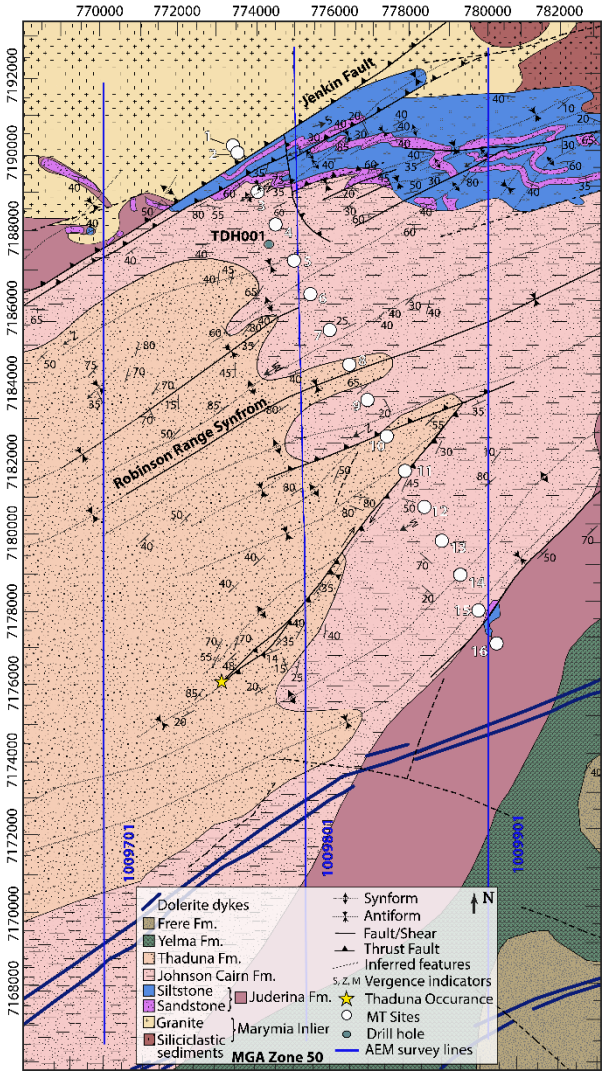

Figure 1. Geological map of the north-eastern Yerrida Basin. MT and AEM survey lines and stations, and interpretated structures and lithologies based on the MT and AEM results in Figures 2 and 3 are annotated.

METHOD AND RESULTS

Magnetotellurics

A 15 km long MT survey line was acquired across the north-eastern Yerrida Basin of the Capricorn Orogen in a northwest to southeast orientation, and located approximately 7 km east of the historic Thaduna copper mine (Figure 1). The survey line covered the sedimentary packages of the deformed TF, JCF and JF, and the northern contact between the Yerrida Basin with the Marymia Inlier (Figure 1).

The MT survey recorded data within both the audio magnetotelluric (10,000 Hz-1 Hz) and broadband magnetotelluric (300 Hz-0.001 Hz) frequency ranges over a minimum time period of 12.5 hrs. The survey was designed with 16 MT stations at 1 km intervals, however, the most northern site of this line was located 250 m from the next closest station (Figure 1) due to the planned location of this station being inaccessible. Overall the survey data was of good quality, however, poor quality measurements were identified within the dead band zone where natural EM fluctuations have a low intensity (1-5 kHz). The processed data produced apparent resistivity and phase data for all stations, of which the majority were 3-dimensional.

The ModEM 3D inversion code (Kelbert et al., 2014) was used to invert the MT data, facilitated by the PAWSEY supercomputing centre Perth, WA. Prior to inversion, spurious data points were manually removed and the number of surveyed frequencies were sub-sampled to reduce the inversion computation time. The final inversion was completed with 24 frequencies and a uniform error floor of 5% for all four components was applied. The final model used a cell size of x: 300 m, y: 300 m and z: 25 increasing by a factor of 1.2, and three additional 50 m wide cells were incorporated between the closely spaced stations 1 and 2. The out of quadrant phases were used within the inversion and included in all iterations. The final inversion results which achieved the best fit between the measured and inverted data required 254 iterations and had an RMS error of 2.28, for frequencies less than 10^3 Hz.

Airborne electromagnetics

The regional-scale TEMPEST AEM survey was acquired at 5 km line-spacing along north-south and east-west survey lines, across the Capricorn Orogen. A single survey line from this regional survey was inverted using the Geoscience Australia 1D inversion algorithm (GA-LEI) (Brodie, 2015). The GA-LEI algorithm is a robust 1D method and has been used extensively for inverting TEMPEST AEM data (Brodie and Fisher, 2008; Hutchinson et al., 2010; Costelloe et al., 2012), and more recently, for creating preliminary AEM inversions from the Capricorn Orogen (Munday et al., 2013). The GA-LEI code simultaneously solves for the AEM system geometry, conductivity, and thickness of each model layer on a sample by sample basis (Brodie, 2015). Additional user defined parameters can be input within the GA-LEI code in the form of a reference model, which directs the inversion towards a preferred model. Within this study, different reference models solving for both the thickness and conductivity of each model layer were applied and ranged from blocky 3-layered inversions to smooth 30-layered inversions. A 30-layered smooth model result for Line 1009801 is presented in this abstract (Figure 3). The inverted result achieved a good fit between the modelled AEM responses and measured AEM data, had a low misfit error for most to the survey stations, and produced resistivity and thickness variations consistent with current geological knowledge of the Yerrida Basin.

MT and AEM comparison

Two cross sections through the final 3D MT model are shown in Figure 2, and a cross-section comprised of the single-station inversion outputs along the AEM Line 1009801 is shown in Figure 3. Within both images, red colours indicate conductive regions, while blue regions represent resistive zones. Annotated on the AEM cross-section are three main conductive regions (C1-C3) and one main resistive region (R1) (Figure 3), and on the MT cross-sections, two main conductors (C1-C2) and two main resistors (R1-R2) have been annotated (Figure 2). In addition, mapped and interpreted faults and fold axes from publicly available field mapping data (Bagas, 1998) have been

annotated in both Figures 2 and 3 (dashed lines with arrows indicating fold axes and fault offsets).

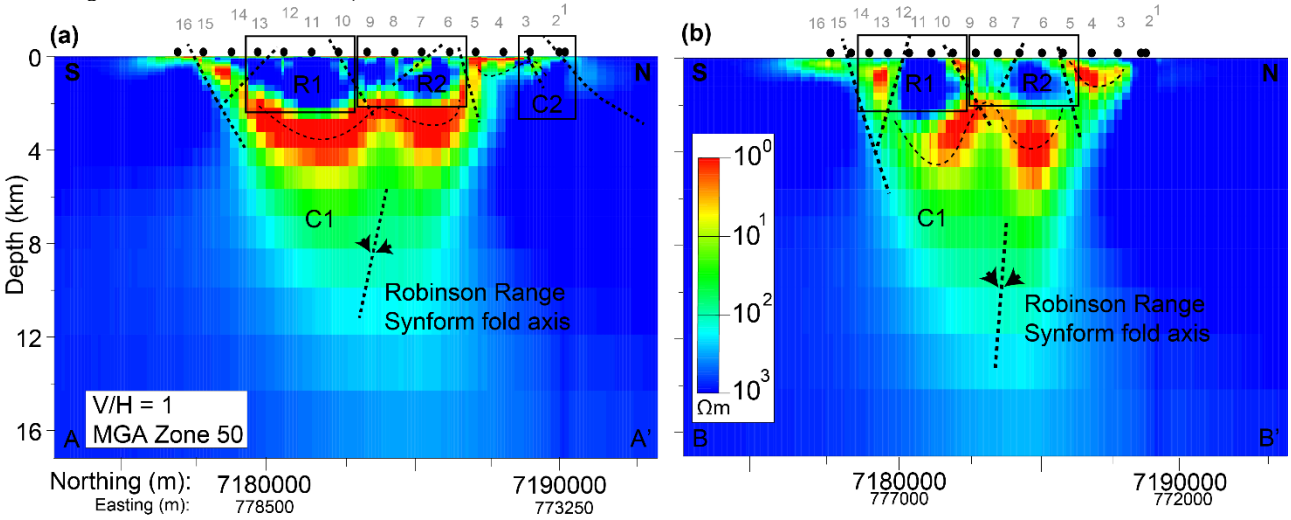

Figure 2. Cross sections through the final Yerrida Basin 3D ModEM MT inversion. Plan view section lines for (a) and (b) are annotated on Figure 1.

Comparisons of the AEM and MT inversions show they have different depths of investigations (DOI), with the MT inversion resolving resistivity and thickness variations to a much greater depth than the AEM inversion. This is not unexpected given the MT survey records a wide range of frequencies which allow for a greater DOI compared to the short range of decay times recorded by the TEMPEST AEM system. With this greater depth of investigation, the km-scale folds associated with the deformation of the conductive JCF by the regional Robinson Range Syncline can be mapped to approximately 4 km to 5 km below the surface (Figure 2, C1). These folds are evident where the highly conductive JCF is in contact with the more resistive units of the younger TF and older JF. In contrast, mapping this scale of deformation from the AEM inversions is more difficult since the TEMPEST AEM system cannot detect these resistivity variations at depths greater than a few hundred metres below the surface. In the AEM results the folded and conductive JCF can be identified at the moderately conductive and north dipping zone in C3, and highly conductive south dipping zone at C1. These features are consistent with a regional synform, however, are less obvious than the folded features in the MT results.

The structures which offset the Yerrida basin formations can be interpreted from both inversion-types where there is sufficient offset of the JCF in the MT inversions, or where a sufficient resistivity contrast is resolved in the AEM and MT inversions. Across the MT inversions, the structures have been interpreted where the conductive JCF is discontinuous, for example, between stations 5 and 7 (Figure 2). However, the faults themselves are not resolved as conductive features within the MT results, therefore it is difficult to map the dip and associated offset of these features where they do not clearly offset the main JCF conductor. In contrast, the AEM inversion recovers a linear north dipping and conductive structural contact between the northern and conductive JCF (C1) and an unexpected moderately conductive JF (C2) (likely associated with the younger and more conductive siltstone and sandstone packages of the JF). This structure is resolved to a depth of approximately 300 m – 450 m below the surface in the AEM inversion and may be a fault splay off the Jenkin Fault. An equivalent feature is not clearly seen in the MT results (Figure 2(a), C2). This may suggest that either this structure is shallow, or is only conductive within the near surface where the conductive JCF and moderately conductive JF sediments are deformed.

The lithospheric-scale contact between the Marymia Inlier and the Yerrida Basin is difficult to interpret. From current geological maps and interpretations (Bagas, 1998; Occhipinti et al., 2017) this contact is likely the Jenkin Fault, however, the dip direction and depth extent of this fault cannot be interpreted where it does not offset lithologies with contrasting resistivities, or where the structure is not conductive itself. Both the MT and AEM results do not resolve an obvious boundary between the Yerrida Basin and Marymia inlier (Figure 2 and 3, between approximately 7190000m – 7192000m). Instead both inversions resolve this contact as a zone of resistivity.

The Thaduna Formation is recovered with similar resistivities in both the MT and AEM results. In the MT inversion the TF is resolved with two near surface resistors (Figure 2(a), R1 and R2), which form an almost continuously resistive zone above the JCF. Similarly, a largely moderately resistive region is recovered at R1 between 7174000 m – 71786000 m in the AEM inversion (Figure 3), which is inconsistent with the graphitic and pyritic shales of the JCF, but consistent with the TF. Both results suggest that the TF may exit across a larger spatial region than current maps indicate (compare cream-brown TF with the pink JCF in Figure 1 and the Figure 3 interpretation). However, it is evident from the MT results that the formation has been structurally deformed and folded (Figure 2(b), R1 and R2). The Thaduna Formation was deposited prior to the deformation by the Robinson Range Synform. Beneath stations 7 to 10 in the MT inversion, the relationship between the TF and JCF becomes more complex where the TF and JCF have been intensely faulted and folded post-deposition.

CONCLUSIONS

The dip direction and depth extent of the basin faults within the Yerrida Basin are difficult to interpret where the lithologies they offset have similar resistivities. The new Yerrida Basin MT inversion presented here does not resolve a dipping conductor coincident with the crustal-scale Jenkin Fault. However, interpretations of the AEM inversions may indicate that a fault splay off the Jenkin Fault has thrust the JF sediments above the highly conductive JCF shales. This features appears to only be conductive within the first 300 m of the surface.

Both electromagnetic inversions have been useful for mapping the basin units across the Yerrida Basin. The MT and AEM inversions show that the TF overlies a much larger area of the northern Yerrida Basin which has previously been considered the JCF (Bagas, 1998). This discrepancy between the mapped and electromagnetic interpretations are not unexpected given the interpretations presented here assume the JCF forms a highly conductive sequence restricted to the graphitic shales in the region; based on recent geological descriptions (Occhipinti et al., 2017) and petrophysical measurements (Banaszczyk, 2019). This is consistent with previous regional-scale MT inversions have which have also recovered the JCF as a highly conductive zone in the northern Yerrida Basin (Dentith et al., (2014) and Piña-Varas and Dentith, (2018a)).

ACKNOWLEDGMENTS

The authors would like to acknowledge the funding provided by the Australian Society of Exploration Geophysicists Research Foundation Grant. This research was carried out while the author was in receipt of a Robert and Maude Gledden Postgraduate Research Scholarship.

REFERENCES

Aitken, A., Banaszczyk, S., Dentith, M., Lindsay, M., Shragge, J., Piña-Varas, P., Annetts, D., Austin, J., Ley-Cooper, Y., Munday, T., et al. 2015. A Major Geophysical Experiment in the Capricorn Orogeny, Western Australia. *ASEG Extended Abstracts* **2015**, 1–5.

Bagas, L. 1998. Marymia, WA Map Sheet 2847 (Western Australia: Geological Survey of Western Australia).

Banaszczyk, S. 2019. Extracting Reliable Geological Information from Electromagnetic Datasets in a Regolith Dominated Terrain: Capricorn Orogen, Western Australia. Phd. The University of Western Australia.

Brodie, R.C. 2015. GALEISBSTDEM: A deterministic algorithm for 1D sample by sample inversion of time-domain AEM data - theoretical details.

Brodie, R.C., and Fisher, A. 2008. Inversion of TEMPEST AEM Survey Data Honeysuckle Creek, Victoria (Canberra: Geoscience Australia).

Brodie, R.C., and Ley-Cooper, A.Y. 2018. AusAEM Year 1 NT/QLD Airborne Electromagnetic Survey (Canberra: Geoscience Australia).

Costelloe, M.T., Roach, I.C., and Hutchinson, D.K. 2012. Frome Embayment TEMPEST AEM Survey: Inversion Report and Data Package (200m) - Version details (Canberra: Geoscience Australia).

Crowe, M., Heinson, G., and Dhu, T. 2013. Magnetotellurics and Airborne Electromagnetics - a combined method for assessing basin structure and exploring for unconformity related uranium. *ASEG Extended Abstracts* **2013**, 1–5.

Dentith, M., Johnson, S., Evans, S., Aitken, A., Joly, A., Thiel, S., and Tyler, I. 2014. A magnetotelluric traverse across the eastern part of the Capricorn Orogen (Western Australia: Department of Mines and Petroleum).

Folkes, C.B. 2017. An integrative approach to investigating crustal architecture and cover thickness in the Southern Thomson region: Modelling new geophysical data (Canberra: Geoscience Australia).

Geoscience Australia 2014. Airborne Electromagnetics (Australian Government; Geoscience Australia). http://www.ga.gov.au/about/projects/resources/continental-geophysics/airborne-electromagnetics#heading-5.

Hutchinson, D.K., Costelloe, M.T., Roach, I.C., and Sorensen, C. 2010. Paterson - TEMPEST AEM survey, Western Australia (Canberra: Geoscience Australia).

Kelbert, A., Meqbel, N., Egbert, G.D., and Tandon, K. 2014. ModEM: A modular system for inversion of electromagnetic geophysical data. *Computers & Geosciences* **66**, 40–53.

Munday, T., Ley Cooper, Y., Johnson, S., and Tyler, I. 2013. A regional scale fixed-wing TDEM survey of the Palaeo-Proterozoic Bryah Basin, Western Australia: Providing insights into a geological setting highly prospective for VMS Cu-Au and mesothermal Au Systems. *ASEG Extended Abstracts* **2013**, 1–4.

Occhipinti, S., Hocking, R., Lindsay, M., Aitken, A., Copp, I., Jones, J., Sheppard, S., Pirajno, F., and Metelka, V. 2017. Paleoproterozoic basin development on the northern Yilgarn Craton, Western Australia. *Precambrian Research* **300**, 121–140.

Piña-Varas, P., and Dentith, M. 2018. 3-D Magnetotelluric Study across the Capricorn Orogen (Western Australia) and its Implications for Mineral Exploration. *Near Surface Geosciences Conference & Exhibition 2018* 1–4.

Pirajno, F., and Occhipinti, S.A. 2000. Three Palaeoproterozoic basins—Yerrida, Bryah and Padbury—Capricorn Orogen, Western Australia. *Australian Journal of Earth Sciences* **47**, 675–688.

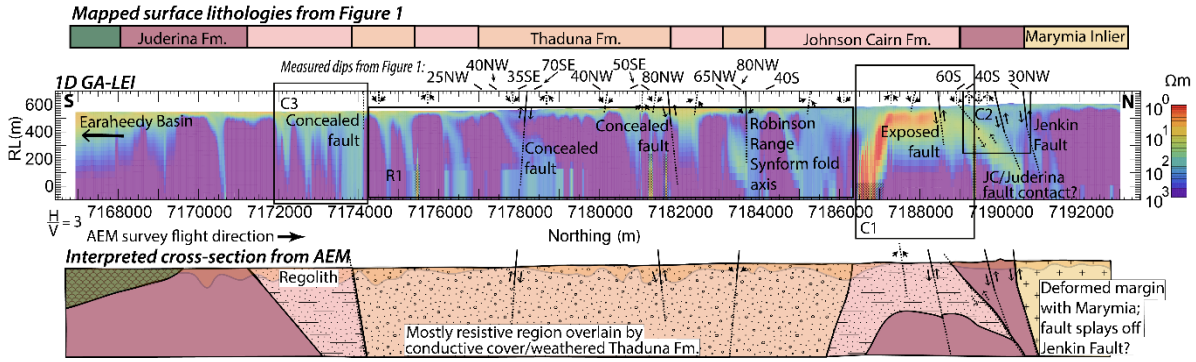

Figure 3. 1D GA-LEI AEM inversion of survey Line 1009801. The geology, dip, and strike measurements (Figure 1) intersected by this line are shown above the inversion. A schematic geological interpretation from the AEM inversion is shown below the inversion output. Regions of high uncertainty have been greyed out on the inverted AEM section.